# BBC Calibration Status in Y2

Takashi Hachiya, Kensuke Homma, Tomoaki Nakamura
Hiroshima University
and
Hiroaki Ohnishi
BNL

September 20, 2001

**Abstract**

In this note, we will report on BBC calibration status in Y2. For Y2 we changed the ADC dynamic range and operational high voltages. As the result of the modification, we succeeded to measure one MIP peaks without obvious overflows in charge measurements in all of 128 PMT's. The intrinsic time resolutions over all PMT's were estimated as $40 \pm 5$ ps. In the current operational condition, we determined a global offset on Z-vertex measurement compared to PC Z-vertex, which has been already applied to constants used for BBLL1.

# Contents

**1 FEM Calibration** **3**
1.1 FEM Modification for Y2 . . . 3
1.2 Pedestal measurements . . . 3
1.3 Measurement of ADC conversion factors . . . 3
1.4 Measurement of TDC conversion factors . . . 4
1.5 Measurement of TDC overflows . . . 5

**2 Gain Calibration** **5**
2.1 Determination of operational high voltages . . . 5
2.2 Measured PMT gains . . . 6

**3 Time Calibration** **8**
3.1 Scheme of slewing correction . . . 8
3.2 Intrinsic time resolution of each Cherenkov element . . . 9
3.3 Effect of operational voltages on the intrinsic time resolutions . . . 9

**4 Global Offset for Z-vertex measurement** **9**

**5 Summary** **15**

# 1 FEM Calibration

## 1.1 FEM Modification for Y2

In Y1, operational voltages were determined so that one MIP corresponds to 80pC in front of FEM input. In order to avoid the overflows in charge measurements seen in Y1 data, we changed the ADC gain for Y2. In addition to the change of the ADC gain, the operational voltages were also reduced so that typically one MIP corresponds to 40 pC for Y2. By this modification, the dynamic range for the charge measurement is expected to be ten times widened compared to Y1. This enables us to measure up to approximately 30 MIP's per PMT as a design value.

Note: In the change of the dynamic range of ADC, the ADC conversion factors were changed from 0.07[pC/ch] to 0.4[pC/ch].

## 1.2 Pedestal measurements

Usually pedestal values can be measured as ADC channels when zero charge is injected. But we can not use this general method, because our ADC is self-gated ADC, that is, the ADC gate does not open until the injected charges exceed a certain threshold. In our setup, pedestal values can be measured based on scanned data by changing DAC (Digital to Analog Converter) values. Figure 1 shows measured ADC channels as a function of DAC values in a typical FEM channel. By extrapolating the slope at the zero DAC value, the pedestal value was determined.

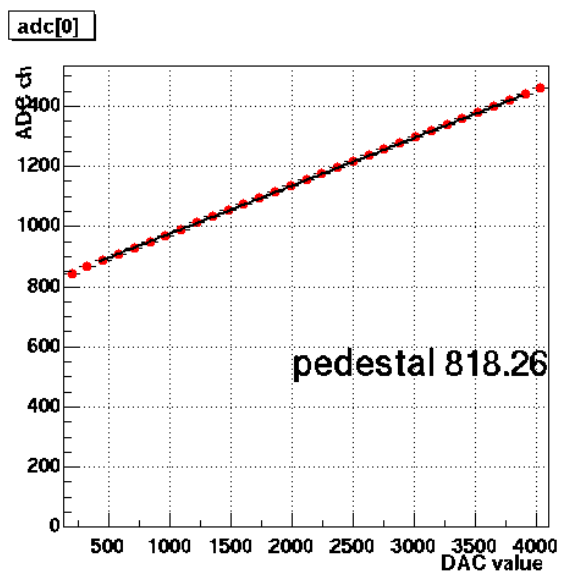


Figure 1: Measured ADC channels as a function of DAC value. Pedestal was obtained by extrapolating the fit line at the zero DAC value.

## 1.3 Measurement of ADC conversion factors

Conversion factors from channels to charge [pC] were estimated by external charge injections. Figure 2 shows measured ADC channels as a function of injected external charges. Those external charge values were determined by charges integrated over 20 ns by using a digital oscilloscope. The inverse slope in Figure 2 corresponds to the conversion factor.

Note: ADC values as a function of DAC value for 128 PMT's can be found in
https://hiroh2.hepl.hiroshima-u.ac.jp/phx/bnl/calibration/Y2/qscan_082201_hist1.ps

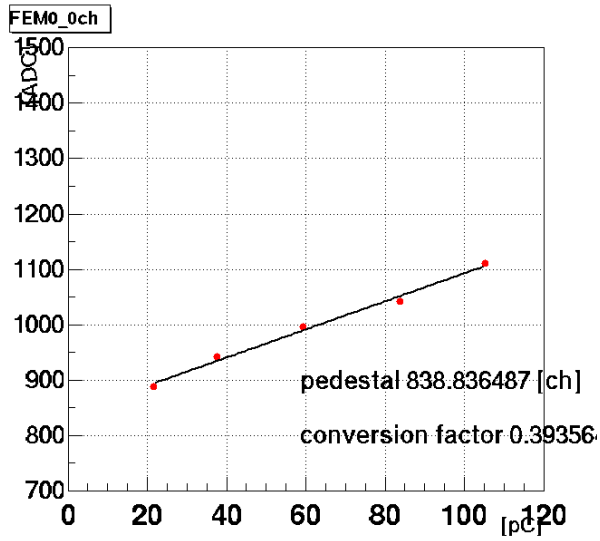


Figure 2: Measured ADC channels as a function of injected charges. Conversion factors were determined by the inverse slope parameter fit with linear function.

## 1.4 Measurement of TDC conversion factors

TDC conversion factors from channel to time [ps] were estimated based on scanned test pulse data by changing delay setting for the test pulse injection. Figure 1.4 shows measured TDC channels as a function of delay setting whose unit is $\frac{4.}{256.} \times$ RHIC clock (106.5805[ns]). The slope was fit with a liner function and it gives us a conversion factor of 7 [ps/ch] typically.

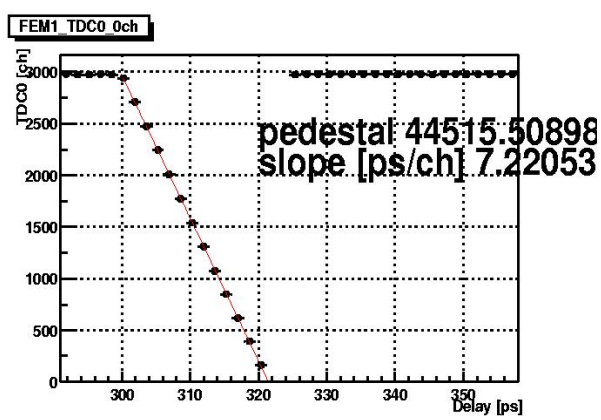


Figure 3: TDC channels distribution as a function of delay setting of test pulses.

Note: TDC values as a function of test pulses delay for 128 PMT's can be found in
https://hiroh2.hepl.hiroshima-u.ac.jp/phx/bnl/calibration/Y2/tscan0_082201_hist.ps
https://hiroh2.hepl.hiroshima-u.ac.jp/phx/bnl/calibration/Y2/tscan1_082201_hist.ps

### 1.5 Measurement of TDC overflows

The overflows in TDC channels are important parameters, since they define whether hits are valid or not. Figure 4 shows a overflow distribution in a typical FEM channel. The typical mean and sigma values are ~3000 ch. and 2 ch., respectively. In BBLL1 algorithm, the valid hit is defined as "TDC $< mean - 6 \times 2$". In offline analysis, we are currently applying a definition "TDC $< mean - 4 \cdot \sigma_{overflow}$".

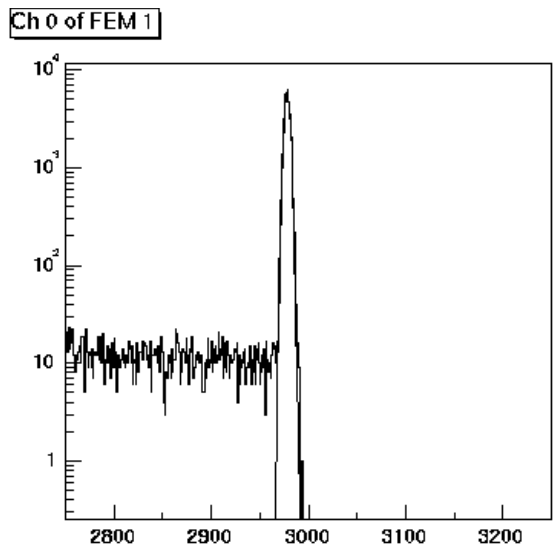


Figure 4: TDC distribution around 3000 [ch]. The peak is the overflow value.

Note: TDC overflow distributions for 128 PMT's can be found in

## 2 Gain Calibration

### 2.1 Determination of operational high voltages

Expected PMT gains were estimated based on one MIP positions obtained in Y1 data together with gain curves of each PMT which were obtained by laser pulse injections. For newly installed PMT's from Y2, one MIP positions were estimated based on cosmic ray data measured at Hiroshima. As an example of determining operational HV, Figure 5 shows a gain curve for a typical PMT where measured charge[pC] is fit with the black curve as a function of supplied HV. This curve was measured by injecting laser pulses which were shared with EMCal, TOF and BBC. The gain curve was fit with an empirical function ;

$$f(HV) = exp(p0 + p1 \cdot HV + p2 \cdot HV^2),$$

where p0, p1 and p2 are parameters.

In order to get absolute scale which provides us optimal operational point, the gain curve is scaled so that Y1 MIP point (86 pC) described by a red dot is on the curve (red line). Based on the curve, the operational point (blue dot on red line) which would produce 40 pC for one MIP was determined. Once we obtained operational points (blue dot) for each PMT, we take an average HV value over typically eight PMT's in a HV group. Finally, we adopt the average value as an operational point (green star) for the HV group. Therefore, expected MIP charges are deviated from the ideal 40 pC among PMT's in the HV group.

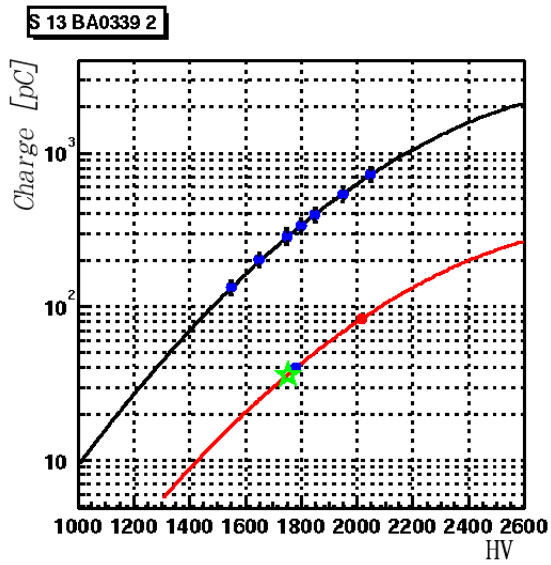


Figure 5: The gain curve of a PMT by laser (black line) and measured MIP position in Y1 data (red dot). Ideal operational HV points (blue dot on red curve) were determined so that one MIP were 40[pC] for each PMT. Expected MIP positions (green star) were calculated by averaging operational HV value over PMT's belonging to the same HV module.

## 2.2 Measured PMT gains

Measured PMT gains were estimated based on one MIP peak positions in Y2 data. The data set used for this study was the following;

- Run 27086
- B field was ON
- Totally 81509 events (11 files) were used before any event selections were applied.

The imposed cuts to get clear one MIP peak positions were following;

- The trigger of "BBCLL1" or "ZDC coincidence" was selected
- TDC values were lower than 2800 not to accept TDC overflow.
- ADC values after pedestals subtraction were greater than 0
- Z vertex positions by BBC were within 20cm
- Total MIP count in Y2 data was lower than 128 in each BBC side.

Figure 6 shows a typical ADC distribution for PMT's in a HV group after pedestal subtraction, where MIP peak positions are fit with Gaussian distribution. In the figure, ADC distributions by requiring valid hits in TDC used for BBLL1 trigger are also overlaid with red histograms. We have two TDC's per FEM channel. One is used for charge measurement, and the other one is used for triggering whose information is used in BBLL1. Since we are applying higher threshold value (-120mV) for triggering purpose compared to charge measurement (-40mV), the overlaid distributions do not have tail parts from electrical noises. As can be seen, the triggered ADC distributions still keep one MIP peak. This guarantees that trigger threshold is properly set and never cause trigger inefficiency to minimum bias events. We are seeing good MIP peaks in all of 128 PMT's and all MIP peaks are kept even in ADC distribution with valid hits in TDC used for BBLL1 trigger. Figure 7 shows the distribution of the MIP peak variation over all 128 PMT's in pC. The average gain is 39 pC for one MIP peak.

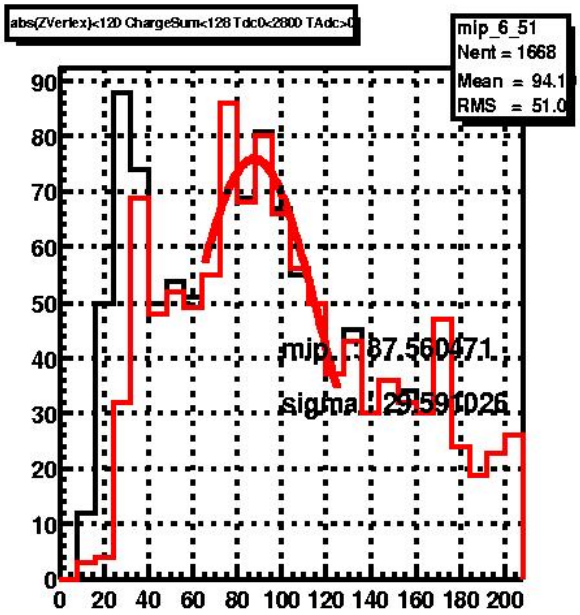


Figure 6: ADC distribution after pedestal subtraction. A MIP is appeared at 87[ch].

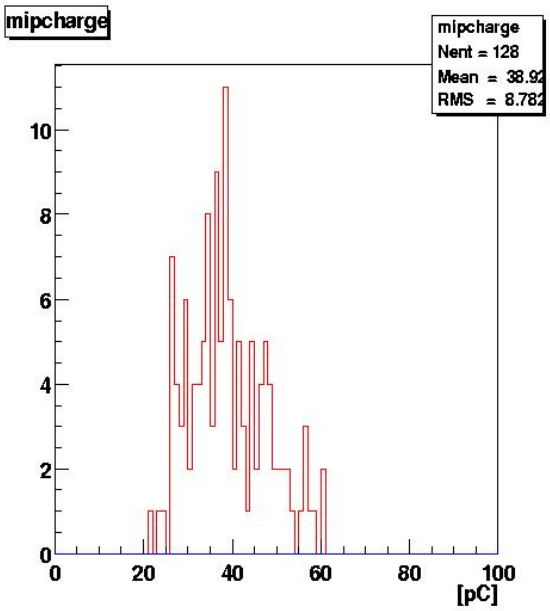


Figure 7: Distribution of the MIP peak variation over all 128 PMT's in pC

Note 1: We have observed ADC overflows in the most inner ring of BBC assemble even in Y2, therefore we decided to supply lower HV for the most inner ring tubes than initially planned, which results 40% reduction of the gain in the lowest gain tube among a HV group but without loosing the MIP peak position.

Note 2: The gain curves for 128 PMT's can be found in
https://hiroh2.hepl.hiroshima-u.ac.jp/phx/bnl/calibration/Y2/HV.ps

Note 3: The ADC distributions used to search MIP peaks for 128 PMT's can be found in
https://hiroh2.hepl.hiroshima-u.ac.jp/phx/bnl/calibration/Y2/mip_100GeV_083001_final1.ps

# 3 Time Calibration

## 3.1 Scheme of slewing correction

For Y2 we will introduce a new parameterization for the slewing function which is parameterized as ,

$$f(x) = a + \frac{b}{ADC} + c \cdot \log(ADC)$$

where a, b and c are constants. In this function, ADC means the value after pedestal values are subtracted. The procedures to get the slewing correction are summarized as follows:

1. Select events which satisfy following conditions;
   - The coincidence between BBLL1 and ZDC was required as trigger selection.
   - Z vertex position was within 20cm.
   - The number of hit pmt was greater than 20.
2. Calculate reference hit time in each BBC side by using non slewing corrected hit time of PMT with valid hit. The definition of "hit" is as follows;
   - Pmtgain was greater than 0.0001.
   - ADC was greater than its pedestal value.
   - TDC was greater than 0.
   - TDC was less than its overflow $-4 \cdot \sigma_{overflow}$.
3. Given a reference hit time per event, the time difference between the reference hit time and hit time of each PMT is measured, and the time difference is plotted with respect to measured charge for each. This is the slewing curve. Once the slewing curve is obtained, the curve is fit with the function above.
4. Given slewing corrected time for each PMT, re-calculate the reference hit time and go back to the procedure 3). At this stage the hit time itself of each PMT is never corrected. Corrected times were used only when calculating reference hit times.
5. Iterate above procedures 3) and 4) five times, since it is necessary to improve time resolution ON REFERENCE HIT TIME.

Firstly we examined following three sorts of reference hit time calculations by looking at a hit time distribution per event where measured times are filled over PMT with valid hit in each side of BBC;

A) Calculate truncated mean time which is currently called "ArmHitTime"

B) Calculate average time in the hit time distribution

C) Calculate peak in the hit time distribution.

Figure 8(top) and (bottom) show accumulated hit time distributions over analyzed events which satisfied multiplicity 0-20 and 60-65 respectively with the same event selections above except cuts on multiplicity. Those accumulated hit time distributions were made so that calculated reference time per event was always set at zero over the entire event sample. Therefore we can estimate how typical hit time distributions look like. As seen in Figure 8(top), we see visible difference between A) and B) in lower multiplicity events. On the other hand, we don't see any large difference between A) and B) in higher multiplicity as in Figure 8 (bottom). C) is obviously worse than the other two. Since A) looks most reasonable, we will always adopt A) as a reference hit time algorithm in the following analysis. Figure 9 shows a slewing curve of a typical Cherenkov element with fit slewing function and Figure 10 shows the corrected slewing curve with the fit function. Figure 11 corresponds to a projection of Figure 10 to the time axis. We will define the sigma in that distribution as the time resolution of the element.

### 3.2 Intrinsic time resolution of each Cherenkov element

Ideally a reference hit time should have an infinite time resolution in order to estimate a pure intrinsic time resolution of each element. Instead of such infinite time resolution, we required charge sum above 600 MIP's in each side in addition to the multiplicity cut of 64 hit PMT's to calculate reference hit time. The attempt of this cut is to get reference hit time as accurate as possible by avoiding ambiguity from time structures of incoming particles and from incomplete slewing corrections as well. Figure 12 shows intrinsic time resolutions over 128 PMT's when we required the additional charge sum cut above, where slewing parameters obtained in section 2 were used. From the figure, the intrinsic time resolution is estimated as $40 \pm 5$ ps.

Figure 13 shows the correlation between intrinsic timing resolutions and reduced $\chi^2$ of fits. From this figure, it is found that intrinsic timing resolutions are not correlated with how well slewing function fit the data. Therefore we should not attribute the variations of intrinsic timing resolutions to how well slewing corrections are made. Figure 14 shows the multiplicity dependence of timing resolution for a typical PMT as an example. This tendency is expected due to the increase of the accuracy on reference hit times and the increase of pulse height in each PMT.

### 3.3 Effect of operational voltages on the intrinsic time resolutions

In case the reduction of operational voltages causes visible worse time resolution, we implemented attenuators before FEM input in two HV groups where higher voltage were supplied while keeping the same gain as in the other tubes with reduced supplied voltages. The blue and red histograms in Figure 12 show time resolution distributions in HV group N4 and S7 respectively, where higher HV values were supplied with attenuators for Y2. No obvious improvements are seen compared to the other PMT's with reduced voltage without attenuators.
Note: 81,509 events of Run 27086 taken with zero magnetic field were used in the analysis above.

## 4 Global Offset for Z-vertex measurement

Since BBC can not provide absolute Z-vertex positions by itself, we need independent Z-vertex measurements from other subsystems in order to determine a global offset on Z-vertex measurement by BBC. As the reference vertex, we used Z-vertex from Pad Chamber which is geometrically adjusted to the center of PHENIX within 1 mm precision. Figure 15 top) shows Z-vertex difference (ZBBC - ZPC) between offline BBC and PC. Figure 15 bottom) shows Z-vertex difference (ZBBCLL1 - ZPC) between BBCLL1 and PC. Based on these figures, the global offset values for both offline BBC and BBCLL1 Z-vertex, in other words, global time offsets were added to both BBC sides so that the average of those two time offsets was canceled out to avoid an additional offset for time zero measurements.

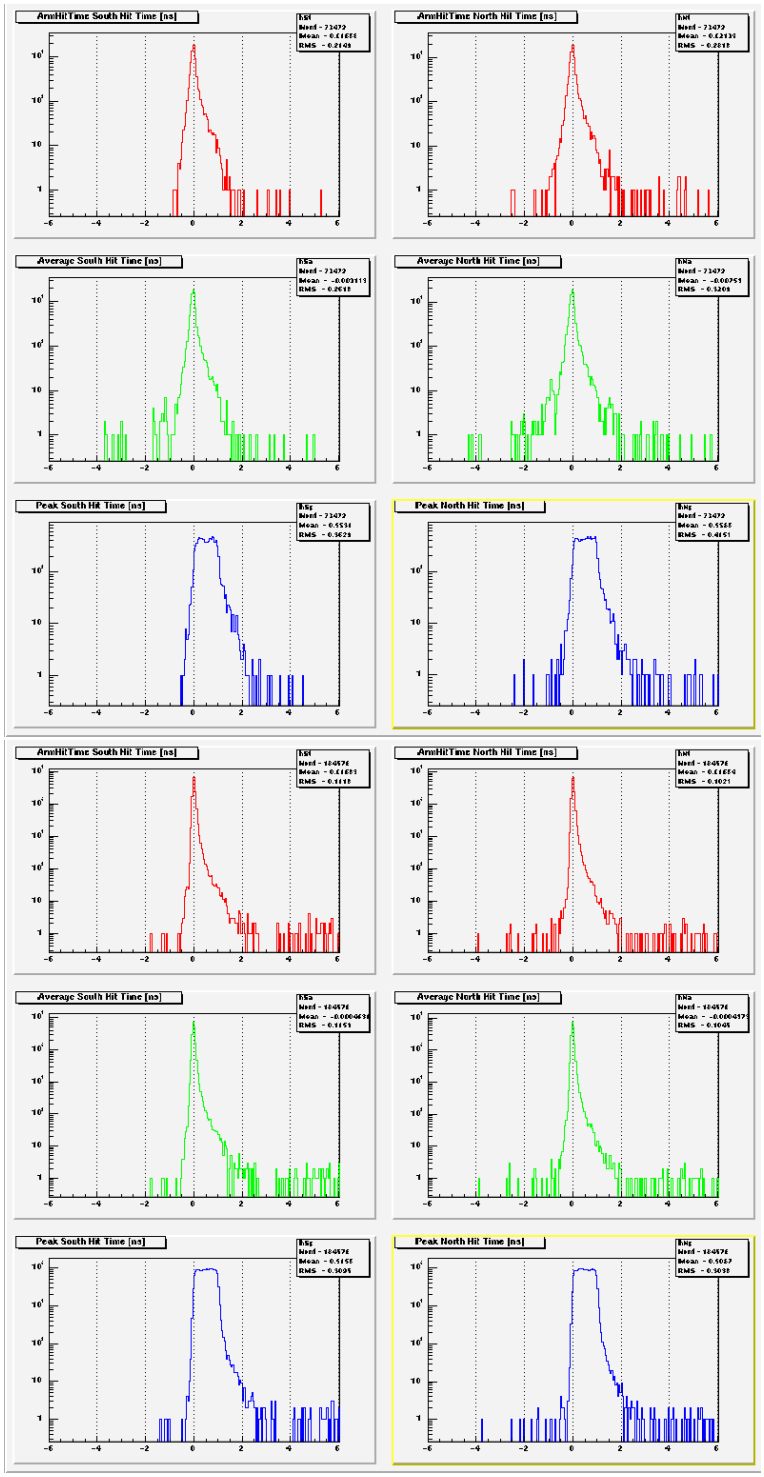


Figure 8: Accumulated hit time distribution with hit multiplicity 0-20(top) and 60-65(bottom). In each figure, left side and right side correspond to South and North BBC, respectively. Red, blue and green histograms are made by using algorithm A), B) and C), respectively.

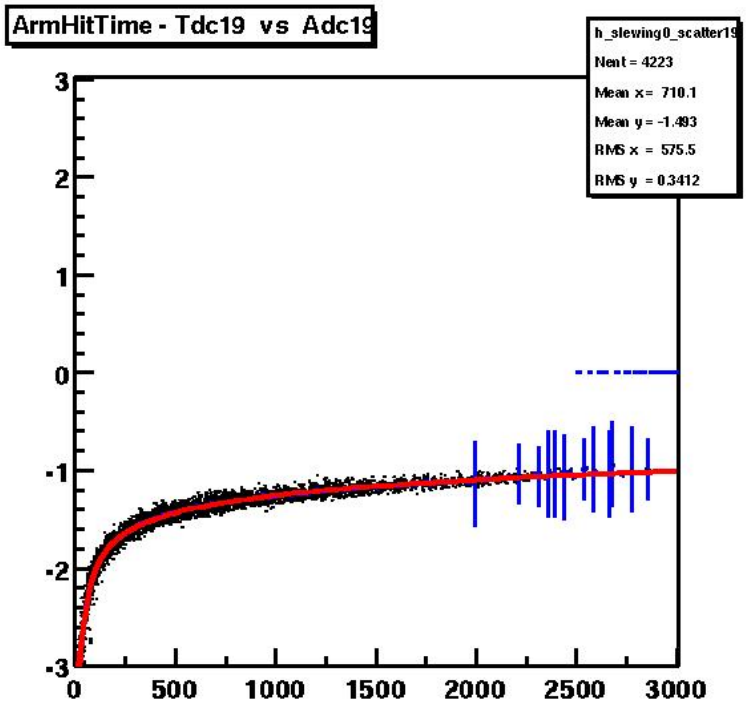


Figure 9: A typical slewing curve overlaid with fit slewing function.

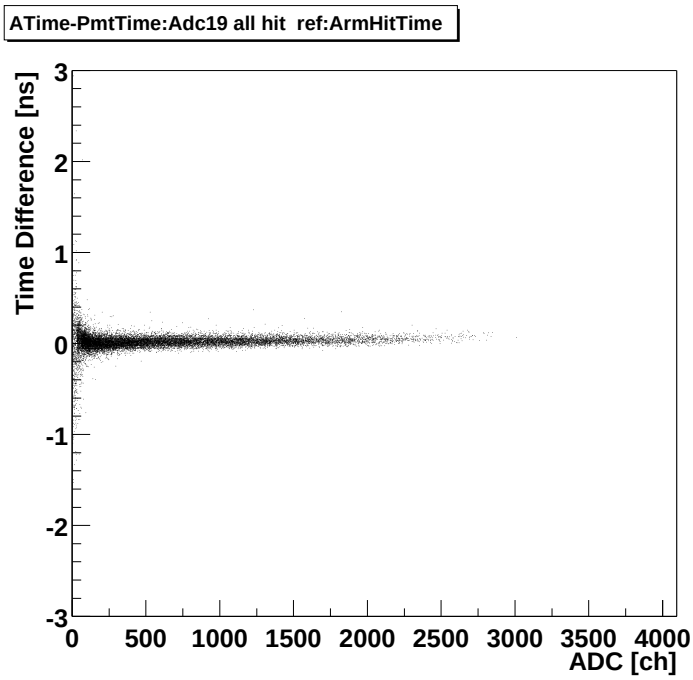


Figure 10: Corrected slewing curve.

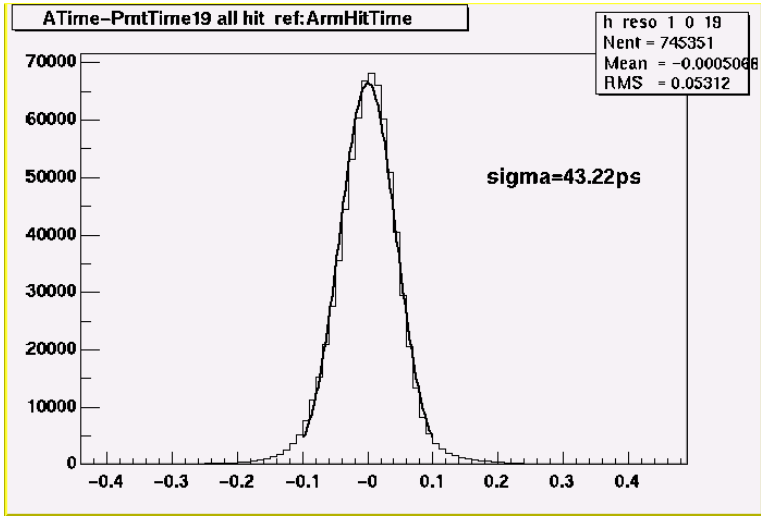


Figure 11: The timing difference between reference time and the corrected timing of a PMT. The sigma of fit function is defined as the timing resolution.

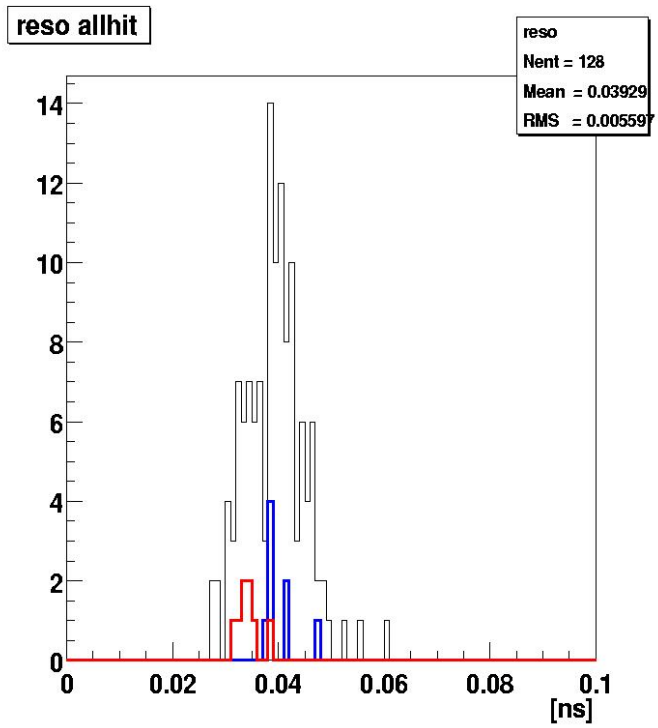


Figure 12: The distribution of timing resolution of all PMT's. The blue and red histograms show time resolution distributions in HV group N4 and S7 respectively, where higher HV values were supplied with attenuators for Y2.

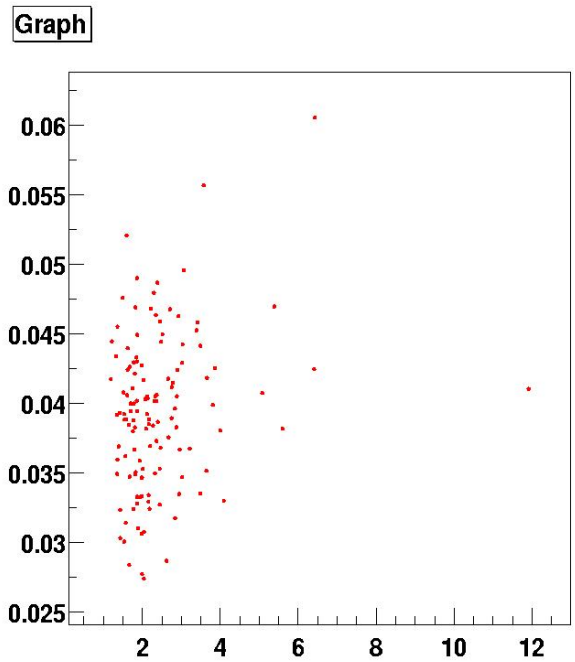


Figure 13: Correlation between intrinsic timing resolutions and $\chi^2$ of hits.

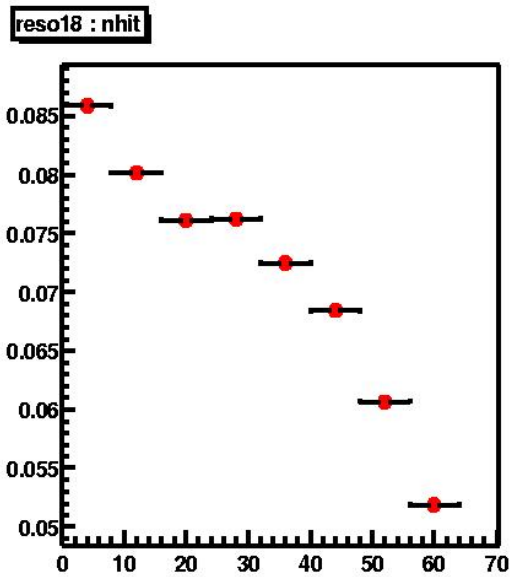


Figure 14: Multiplicity dependence of time resolutions for a typical PMT as an example

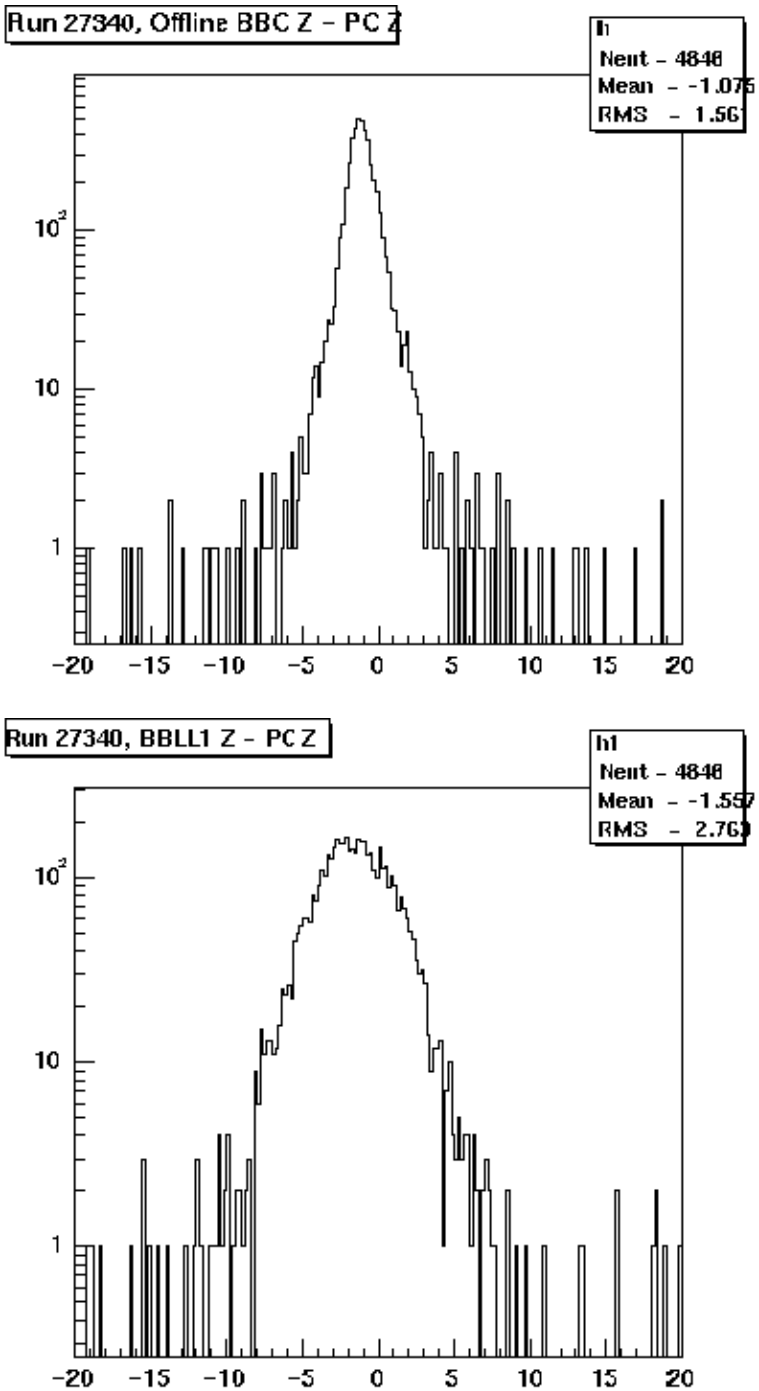


Figure 15: top) shows Z-vertex difference (ZBBC - ZPC) between offline BBC and PC. bottom) shows Z-vertex difference (ZBBCLL1 - ZPC) between BBCLL1 and PC

# 5 Summary

We could identify clear one MIP peaks in all of 128 PMT' for Y2. We do not have obvious overflow in ADC channels for Y2. The average gain value is 39 pC and 32 pC for the most inner tubes for one MIP peaks in the final HV configuration.

Trigger threshold is properly set so that it keeps one mip peak positions with valid TDC hits for triggering.

It was found that the truncated mean time (ArmHitTime) was well established algorithm to estimate a reference hit time which is more robust compared to a simple average on hit times especially in lower multiplicity events. The pure intrinsic time resolution is expected to be below $40 \pm 5$ ps. We need to wait for information from more accurate independent subsystem. There is no significant difference on the time resolution between PMT's with higher HV with attenuators and ones with reduced HV without attenuators.

Global Z-vertex offset has been determined so that BBC offline vertex coincides with PC Z-vertex which is adjusted to the center of PHENIX geometrically. The online (BBLL1) vertex has also been adjusted to the BBC offline vertex, there fore the absolute vertex cut in BBLL1 exactly matches real vertex positions in its mean value.